PROCESS INTENSIFICATION FOR THE SMALL FOOTPRINT COMPACT HEAT TRANSFER DEVICE

Jogender Singh*, Rishabh Aggarwal, Sarvesh Palwal, Dhananjay Kumar Pal, Sandeep Kumar, Kanika Meena and Ankush Jindal.
*Author for correspondence
Department of Chemical Engineering,
National Institute of Technology,
Hamirpur, 177005,
India,
E-mail: jogender8295@gmail.com

ABSTRACT

Process intensification for the development of compact heat exchanger with small footprint is greatest challenge of the heat exchanger technology today. In the present study, a heat transfer device, coiled flow inverter (CFI) is revamped for the better heat transfer efficiency with a smaller footprint. The proposed small foot-print coiled flow inverter (SFCFI) is fabricated by bending of helical coil at 90° with equal arm lengths before and after the bend with variable curvature radius. In integration to the improved centrifugal force due to variable curvature, the SFCFI additionally offers a complete 90° flow inversion caused by each 90° bend, which results in higher radial mixing and heat transfer. The velocity and temperature flow fields depict the improved radial mixing under the laminar flow regime for the Dean number ranges from 8 to 1581. The performance of existing CFI of same heat transfer area (0.17 m^2) was studied and compared with the novel SFCFI device. The results suggest, the proposed SFCFI device provides three-fold heat transfer enhancement as compared to the straight tube of same heat transfer area at Dean number 400. Additionally, heat transfer coefficient in SFCFI enhanced by 48 % as compared to helical coil. Furthermore, SFCFI provides 18 % higher value of Nusselt number as compared to the CFI. The reason for improved heat transfer may be the enhanced centrifugal force due to additional curvature effect provided in each arm of SFCFI in the plane of vortex formation. It was interesting to note that the proposed device provides 11 % lower pressure drop as compared to the CFI. The present study may aids to the development of a novel design of compact coiled and small footprint heat transfer device.

INTRODUCTION

Heat exchangers are the integral part of the various heat consuming processes in the different industries such as automotive industries, oil and gas industries, aerospace, biomedical, cement and chemical industries.

NOMENCLATURE

A	[m^2]	Heat transfer area
Cp	[kJ/kgK]	Specific heat
Dc	[mm]	Curvature diameter
d_i	[mm]	Tube diameter
k	[W/mK]	Thermal conductivity
N_b	[-]	Number of 90° bends
h	[W/m^2K]	Heat transfer coefficient
Nu	[-]	Nusselt number ($\frac{h\,di}{k}$)
p	[N/m^2]	Pressure
Pt	[m]	Pitch
q_w	[W/m^2]	Heat flux
T_o	[K]	Temperature
u_o	[m/s]	Uniform axial velocity
u_i	[m/s]	Velocity component in i-direction (i = 1,2,3)
g	[m/s^2]	Gravitational acceleration
l	[m]	Length of geometry
f	[-]	Friction factor
μ	[kg/ms]	Dynamic viscosity
λ	[-]	Curvature ratio (ratio of Dc and d_i)
ρ	[kg/m^3]	Density of fluid
Re	[-]	Reynolds number ($\frac{\rho\, u_i\, d_i}{\mu}$)
De	[-]	Dean number ($\frac{Re}{\sqrt{\lambda}}$)

Greek symbols

θ	[-]	Helical coordinate in the circumferential direction
φ	[°]	Angle (measure of axial position)
δ	[-]	Dirac delta function

Subscripts

o	Inlet conditions
w	Wall condition

The conventional heat transfer technologies such as shell and tube, plate and frame and fin tube heat exchangers have reached to its limitation of heat transfer augmentation. The bent geometries such as L, Y and T bend provide better heat transfer as compared to conventional straight tube technologies [1, 2].

Furthermore, the curved geometries such as spiral, helical pipes were found more effective than bent technologies [3-9]. Though, the conventional heat exchanger geometries provide good heat transfer but require higher energy, material and space. Therefore, the process intensification is today's need to develop a heat exchanger technology with the reduced cost, space and material. The innovative work of Dean for conventional size curved pipe leads to the several investigations for the fundamental understanding of heat transfer and flow behaviour in curved channels such as bent, spiral and helical coils [3, 4]. The curved channels results in the better mixing as compared to the conventional channels specifically when arranged in such a manner that chaotic flow patterns are induced [5, 6]. In curved channels, the secondary flow develops with increase in Dean number due to enhanced centrifugal forces, however the secondary flow is insignificant at lower values of Dean number [7]. The friction factor in curved channels increases with the decrease in the curvature radius due to enhanced centrifugal forces [8]. In curved channels, heat transfer rate depends on Reynolds and Prandtl number along with different geometrical design parameters [9]. It was reported that better heat transfer performance can be achieved by parting and redirecting the fluid in bent geometries [10, 11]. The previous study for coiled flow invertor (CFI) shows that CFI provides up to 13.7 % increase in heat transfer coefficient as compared to the straight tube [12]. CFI was fabricated by bending the helical coils of equal arm lengths at 90°, emerged as a new compact three dimensional device in the heat exchanger technology [21]. In comparison to the helical coil, CFI delivers enhanced mixing and much higher heat and mass transfer with negligible increase in pressure drop under laminar flow conditions [12-19]. MCFI offers up to 14% higher conversion in comparison to other capillary setups for a gas-liquid reaction system [22]. Micro-flow extraction process offers faster extraction, higher extraction ability for Co, lower extraction for Ni, and better selectivity between Co and Ni as compared to batch extraction [23].

Geometry perturbation is one of the promising and radical technology to augment the heat transfer coefficient. In the present study, CFI is revamped for the higher heat transfer efficiency and smaller foot print. The proposed device small footprint coiled flow invertor (SFCFI) is provided with extra curvature in each of its equal arms as shown in Figure 1(a). Numerical investigation has been performed for heat transfer performance of both the devices, CFI and SFCFI with tube diameter 10 mm and curvature diameter 100 mm under laminar flow conditions. The Dean number is varied from 8 to 1581 (Re = 26 to 5000). The heat transfer performance of the four different geometries i.e. straight tube, helical coil, CFI and SFCFI of the same heat transfer area (0.17 m^2) have been investigated and compared. The details of all geometries have been shown in Figure 1.

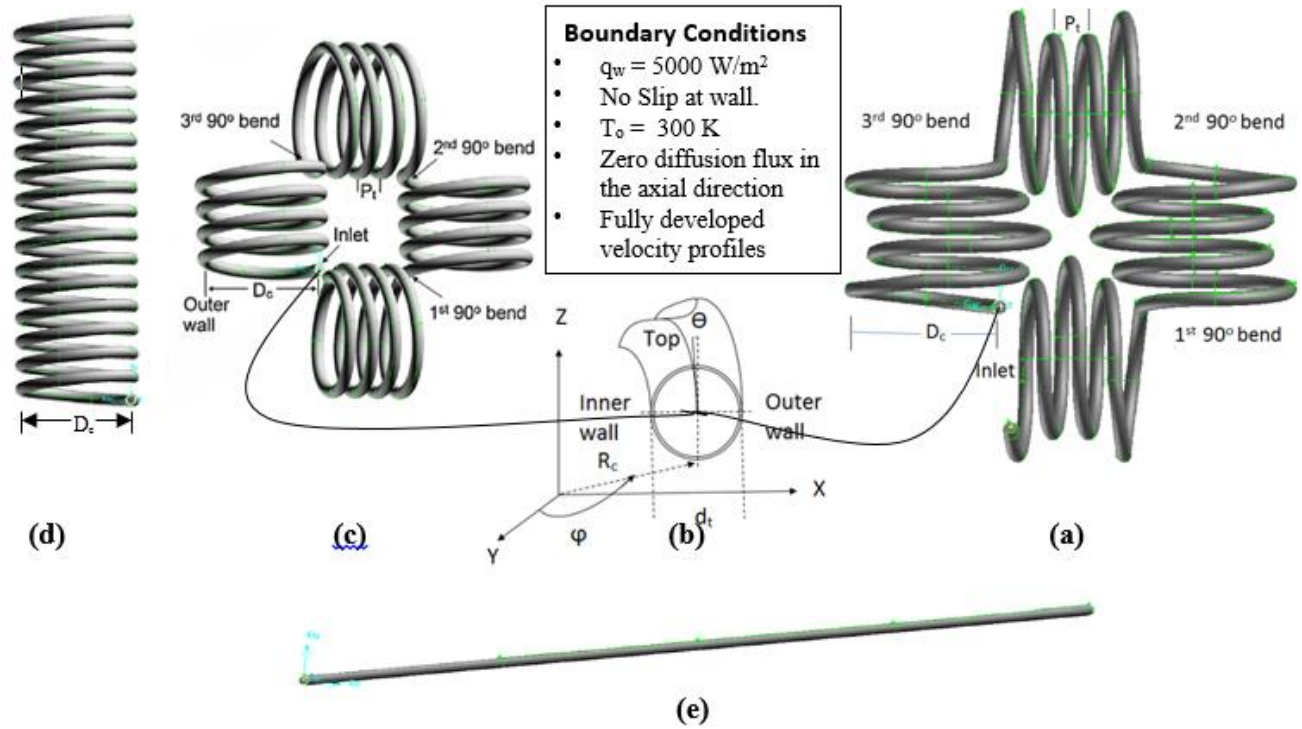

Figure 1. The geometries (a) SFCFI (b) the systemof coordinates considered for numerical simulation (c) CFI and (d) Helical coil (e) Straight tube

MATHEMATICAL FORMULATION

In the present study four different geometries of same heat transfer area have been considered to investigate the simultaneous effect of flow inversion and centrifugal force. Four different geometries are shown in Figure 1(a),(c),(d),(e). The coordinate system is shown in Figure 1(b). To discretize the computational domain a structured non-uniform grid is considered as shown in Figure 2. SIMPLEC scheme is used for pressure-velocity coupling, where as a second order upwind method is used for the diffusive and convective terms. Different grid sizes have been used to assure the grid independency of the results as shown in Figure 3. The optimized grid size is selected for the present calculations. The selected grid independent solution was observed at mesh size of 2868627 hexahedral cells as shown in Figure 3.

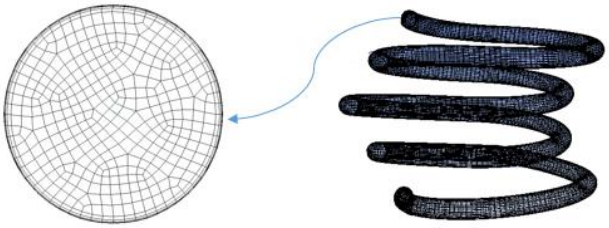

Figure 2. Grid topology used to discretize the model equations.

Stainless steel was taken as the material of construction for the tube. Control volume finite difference method (CVFDM) was used for the numerical analysis of all four geometries.

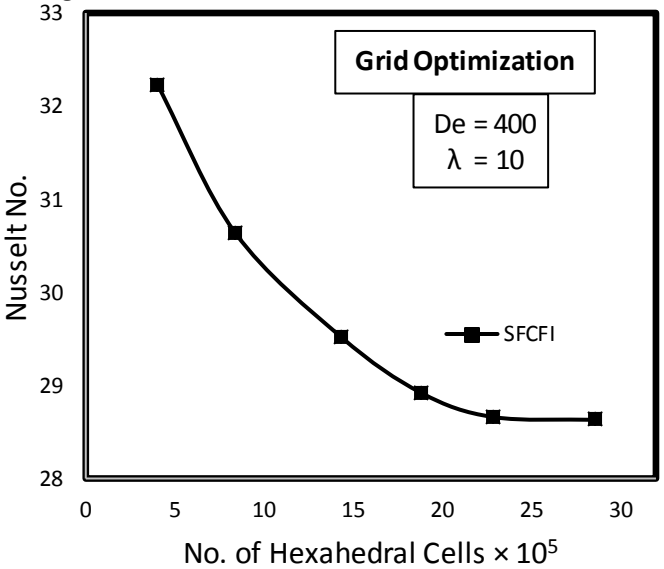

Figure 3. Variation of Nu with the number of hexahedral cells for grid optimization in SFCFI.

The mesh configuration and geometric details are given in Table 1 and Table 2 respectively. Fluid properties are assumed to be independent of thermophysical properties.

Laminar flow model is considered. The absolute convergence criterion is taken as follows,

$$\frac{R_\phi^m}{R_\phi^n} \le 10^{-6}$$

Where, R_ϕ^n represents the maximum residual value of ϕ variable after n iterations and is applied for p, u_i, T and the residual summed up over all computational nodes at the m^{th} iteration is R_ϕ^m.

Table 1. Details of mesh configuration

Nodes	3017322
Hexahedral cells	2868627

Table 2. Details of the geometries

	CFI	SFCFI
d_i (mm)	10	10
D_c (mm)	100	100
Λ	10	10
l (m)	5.34	5.34
P_t (mm)	20	24
Total no. of turns	16	16
N_b	3	3
A (m^2)	0.17	0.17

GOVERNING EQUATION

The governing equations of mass, momentum, energy were solved by using commercial software ANSYS Fluent 12.1. The steady state flow has been considered. The governing Navier–Stokes and energy equation for the laminar flow and heat transfer in a coiled configuration [13] are given below.

Continuity equation for constant density

$$\frac{\partial u_i}{\partial x_i} = 0$$

Momentum equation

$$\frac{\partial}{\partial x_i}\left[\mu\left(\frac{\partial u_i}{\partial x_j}+\frac{\partial u_j}{\partial x_i}\right) - \rho u_j u_i - \delta_{ij} p\right] + \rho g_i = 0$$

Energy equation

$$\frac{\partial}{\partial x_j}\left[k\left(\frac{\partial T}{\partial x_j} - \rho u_j C_p T\right) + \mu\phi_v\right] = 0$$

Where $\mu\phi_v$ is the viscous heating term and ϕ_v is given by

$$\phi_v = \frac{\partial u_i}{\partial x_j}\left(\frac{\partial u_i}{\partial x_j}+\frac{\partial u_j}{\partial x_j} - \frac{2}{3}\mu\frac{\partial u_i}{\partial x_j}\delta_{ij}\right)$$

BOUNDARY CONDITIONS

Uniform heat flux (q_w = 5000 W/m^2) and no slip condition were imposed on the tube wall. Fully developed velocity profiles at the tube exit were employed. The uniform axial velocity u_o and temperature T_o (300 K) were assumed at the tube inlet. Zero diffusion flux in the axial direction was assumed.

RESULTS AND DISCUSSION

The present computation technique was checked and validated for its accuracy and reliability by regenerating the results for CFI in the available literature [21] as shown in Figure 4. The all four considered geometries viz. straight tube, helical coil, CFI and SFCFI are of same heat transfer area (0.17 m^2).

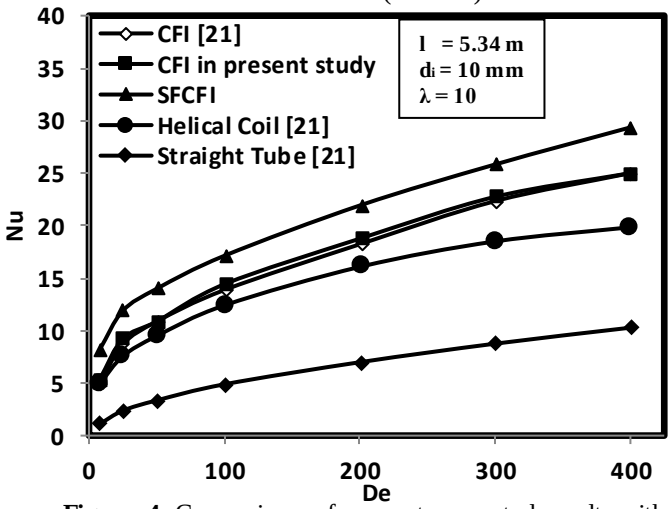

Figure 4. Comparison of present computed results with numerical results available in the literature for CFI, Helical coil and Straight tube.

The numerically computed results are in good agreement with the results reported in the literature [21]. The Dean number is in the range of 8 to 1581. The Nusselt number for the present computational results are compared with CFI, helical coil and straight tube, available in the literature [21] and is shown in Figure 4. Figure 4 clearly depicts that the heat transfer enhancement in SFCFI is 186%, 48%, 18% higher as compared to straight tube, helical coil and CFI respectively. This may be due to the reason of extra curvature effect in the SFCFI in each of its equal arms. The Nu variation with change in the value of De is plotted in Figure 5.

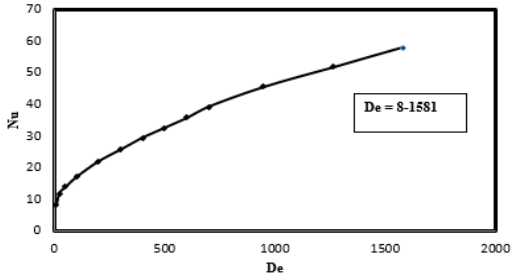

Figure 5. Variation of Nu with De (8 to 1581) in SFCFI

VELOCITY PROFILE

Velocity profiles at outlet of the SFCFI in x, y directions for various values of De within the range of 8 to 1581 are shown in Figure 6. It may be observed from Figure 6 that the centrifugal force increases with increase in the value of De and also the outlet velocity is 62.3% (inlet velocity = 0.222423 m/s, outlet velocity = 0.36099 m/s) higher as compared to inlet velocity. The Dean vortices clearly appear at higher values of De. The reason behind this is the reducing effect of the centrifugal force at lower value of De. This is due to the insufficient centrifugal force to overcome the stream wise inertia. The movement of the fluid in the central region of SFCFI appears to be enhanced with additional development of the vortex towards the outer wall. Here, the inner wall corresponds to the wall towards the centre of curvature of geometry and the outer wall is the wall of the tube opposite to the centre of curvature.

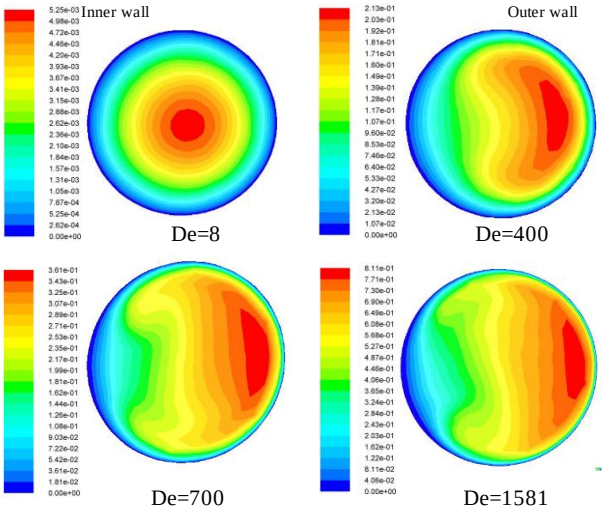

Figure 6. Velocity profiles at the outlet of SFCFI at different values of De.

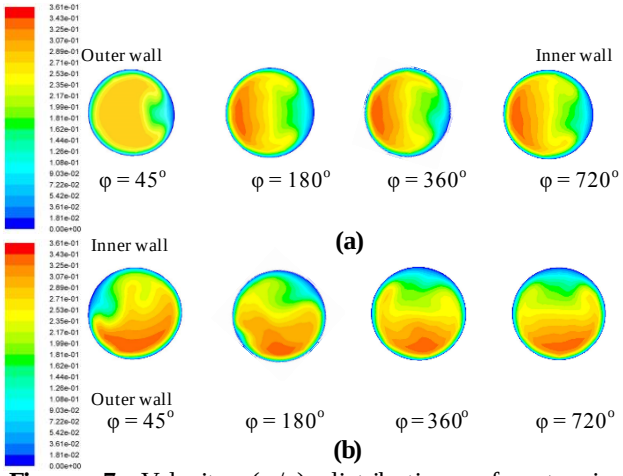

Figure 7. Velocity (m/s) distributions of water in different axial planes of SFCFI at De = 700. (a) before 1st 90° bend (b) after 1st 90° bend.

The velocity contours of the SFCFI for De = 700 at different values of the circumferential angle (φ), which is a measure of axial position, are shown in Figure 7 (a), (b). The axial length in SFCFI increases with increase in the value of φ. Figure 7 (a) shows that effect of secondary flow is lower for the smaller axial length and increases with increase in axial length. Figure 7 (b) shows the

phenomenon of flow inversion caused by the 90° bend, which results in higher radial mixing and heat transfer.

TEMPERATURE PROFILE

Temperature contours are plotted at different angular planes (circumferential angle (φ)) of SFCFI at De = 700 and are shown in Figure 8 (a), (b). Formation of Dean Vortices are clearly visible as axial length increases. Heat transfer rate increases with decrease in the distance between the heat source and heat sink. Figure 8 (a) clearly depicts that high temperature zone shifts towards the outer wall due to the action of centrifugal force in the device which results into better heat transfer. The thermal boundary layer develops with the increase of axial length. Thus secondary convection drives the hot material into the fluid core. Figure 8 (b) shows that plane of vortex formation rotates to an angle of 90°. Reason behind this is the change in the direction of centrifugal force acting normal to the direction of fluid flow. Thus due to enhanced radial mixing high thermal performance is achieved.

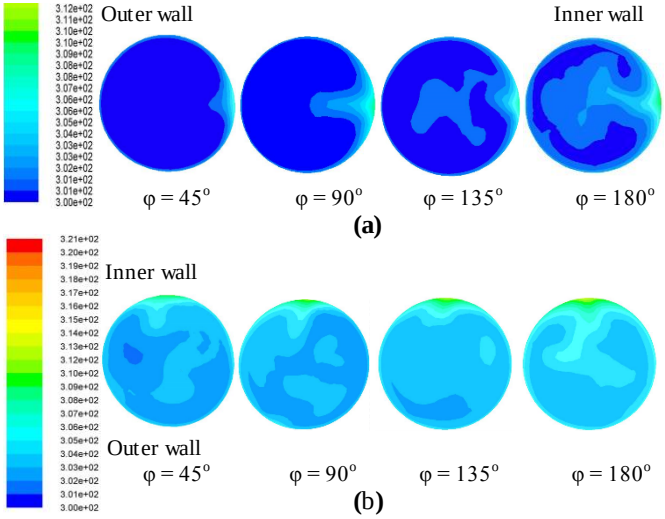

Figure 8. Temperature (K) distributions of water in different axial planes of SFCFI at De=700. (a) before 1st 90° bend (b) after 1st 90° bend.

FRICTION FACTOR

Performance of the SFCFI is measured by comparing the value of friction factor for fully developed flow in CFI of equal length and diameter. Figure 9 shows that the friction factor for SFCFI is in good agreement with the numerical results of CFI, helical coil and straight tube available in literature. Friction factor decreases with increasing De for all four geometries [21] as shown in Figure 9. This is due to decrease in shear stress as velocity gradient increases with increase in Dean number. The friction factor in SFCFI is marginally (up to 11 %) lower as compared to CFI for the De ranging from 8 to 1581, at a given tube diameter (10 mm). The decrease in friction factor may be due to the formation of weaker velocity gradients in each of its equal arms caused by enhanced centrifugal force.

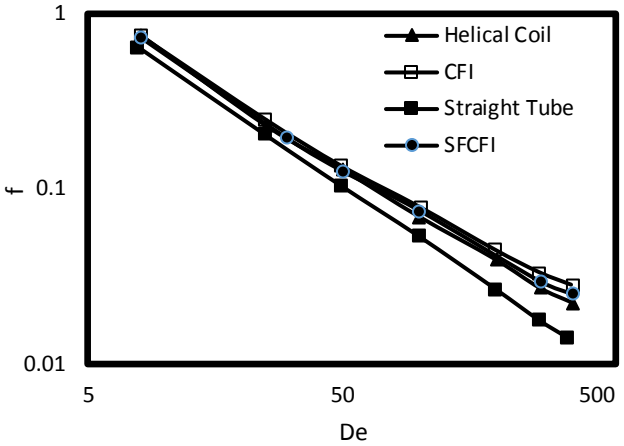

Figure 9. Effect of De on f in geometries under consideration.

CONCLUSION

The present study investigates the hydrodynamics and heat transfer in a novel device SFCFI, along with straight tube, helical coil and CFI heat exchangers of same heat transfer area (0.17 m^2). The Dean number was in the range of 8 to 1581. The heat transfer results revealed that the proposed SFCFI device offers higher value of Nu as compared to all other three geometries considered in the present study. The Nu in the CFI was found to be three times to that of straight tube for De = 400. The Nu further enhanced by 48% in SFCFI as compared to helical coil at De = 400, with relative 11% decrease in the friction factor. In addition, the SFCFI offers 18% enhancement in Nu as compared to CFI of the same heat transfer area. Thus, the modelling efforts in the present work should motivate to develop truly novel three-dimensional devices for practical applications in various fields.

REFERENCES

[1] Prasun D., Sumit K.S., Nrityananda N., Nairit P., Numerical study on flow separation in 90° pipe bend under high Reynolds number by k-ε modelling, Engineering Science and Technology, an International Journal, Volume 19, Issue 2, June 2016, Pages 904–910.

[2] Balvinder S., Harpreet S., Satbir S.S., CFD analysis of fluid flow parameters within a Y-Shaped branched Pipe, International Journal of Latest Trends in Engineering and Technology (IJLTET).

[3] W.R. Dean, Note on the motion of fluid in a curved pipe, Philos. Mag. 4 (1927) 208–223.

[4] W.R. Dean, The streamline motion of fluid in a curved pipe, Philos. Mag. 5 (1928) 673–695.

[5] F. Schönfeld, S. Hardt, Simulation of helical flows in microchannels, AIChE. J. 50 (2004) 771–778.

[6] N. Kockmann, D.M. Roberge, Transitional flow and related transport phenomena in curved microchannels, Heat Transfer Eng. 32 (2011) 595–608.

[7] S. Kim, S.J. Lee, Measurement of Dean flow in a curved micro-tube using micro digital holographic particle tracking velocimetry, Exp. Fluids 46 (2009) 255–264.

[8] W.H. Yang, J.Z. Zhang, H. Cheng, The study of flow characteristics of curved microchannel, Appl. Therm. Eng. 25 (2005) 1894–1907.

[9] X.F. Peng, G.P. Peterson, Convective heat transfer and flow friction for water flow in microchannel structures, International Journal Heat Mass Transfer 39 (1996) 2599–2608.

[10] H.A. Mohammed, P. Gunnasegaran, N.H. Shuaib, Numerical simulation of heat transfer enhancement in wavy microchannel heat sink, Int. Commun. Heat Mass 38 (2011) 63–68.

[11] H.D. Baehr, K. Stephan, Warme- und Stoffubertragung, Springer-Verlag, Berlin, 2004.

[12] M.M. Mandal, V. Kumar, K.D.P. Nigam, Augmentation of heat transfer performance in coiled flow inverter vis-a-vis conventional heat exchanger, Chem. Eng. Sci. 65 (2010) 999–1007.

[13] A.K. Saxena, K.D.P. Nigam, Coiled configuration for flow inversion and its effect on residence time distribution, AIChE J. 30 (1984) 363–368.

[14] V. Kumar, K.D.P. Nigam, Numerical simulation of steady flow fields in coiled flow inverter, International Journal Heat Mass Transfer 48 (2005) 4811–4828.

[15] V. Kumar, M. Mridha, A.K. Gupta, K.D.P. Nigam, Coiled flow inverter as a heat exchanger, Chem. Eng. Sci. 62 (2007) 2386–2396.

[16] M. Mridha, K.D.P. Nigam, Coiled flow inverter as an inline mixer, Chem. Eng. Sci. 63 (2008) 1724–1732.

[17] J. Singh, V. Verma, K.D.P. Nigam, Flow characteristics of power-law fluids in coiled flow inverter, Ind. Eng. Chem. Res. 52 (2013) 207–221.

[18] J. Singh, N. Kockmann, K.D.P. Nigam, Novel three-dimensional microfluidic device for process intensification.

[19] F. Kopf, M. Schlüter, D. Kaufhold, L. Hilterhaus, A. Liese, C. Wolff, S. Beutel, T. Scheper, Laminares mischen in miniatur-hohlfasermembranreaktoren durch ausnutzung von sekundärströmungen (teil 1), Chem. Ing. Tech. 83 (2011) 1066–1073.

[20] D. Kaufhold, F. Kopf, C. Wolff, S. Beutel, L. Hilterhaus, M. Hoffmann, T. Scheper, M. Schlüter, A. Liese, Reaktive absorption von kohlenstoffdioxid in helikalen hohlfasermembrankontaktoren, Chem. Ing. Tech. 85 (2013) 476–483.

[21] J. Singh, N. Choudhary and K.D.P. Nigam, The Thermal And Transport Characteristics of Nanofluids in a Novel Three-Dimensional Device.

[22] S. K. Kurt, F. Warnebold, K D.P. Nigam, N. Kockmann, Gas-Liquid Reaction and Mass Transfer in Microstructured Coiled Flow Inverter.

[23] Zhang, Lihua, Hessel, V, Peng, Jinhui, Wang, Q. & Zhang, Libo (2017), Co and Ni extraction and separation in segmented micro-flow using a coiled flow inverter.